

Automatized Search for Complex Symbolic Dynamics with Applications in the Analysis of a Simple Memristor Circuit

Zbigniew Galias

*Department of Electrical Engineering,
AGH University of Science and Technology,
Mickiewicza 30, 30-059 Kraków, Poland
galias@agh.edu.pl*

An automatized method to search for complex symbolic dynamics is proposed. The method can be used to show that a given dynamical system is chaotic in the topological sense. Application of this method in the analysis of a third-order memristor circuit is presented. Several examples of symbolic dynamics are constructed. Positive lower bounds for the topological entropy of an associated return map are found showing that the system is chaotic in the topological sense.

Keywords: Chaos; symbolic dynamics; topological entropy; memristor circuit; interval arithmetic.

1. Introduction

We say that a dynamical system is chaotic in the topological sense if its topological entropy is positive. This can be shown by proving that there exist a horseshoe type chaos for the system, i.e. that there exist sets supporting symbolic dynamics with positive topological entropy.

One of the frequently used methods to prove the existence of symbolic dynamics of a certain type is based on the notion of covering relations [Zgliczyński, 1997]. This method has been successfully used to prove the existence of topological chaos for a wide class of discrete systems [Zgliczyński, 1997; Galias & Zgliczyński, 2001] and continuous systems [Zgliczyński, 1997; Galias, 1997; Galias & Zgliczyński, 1998; Arioli & Zgliczyński, 2001; Wilczak, 2003]. Usually, sets supporting complex symbolic dynamics are found by trial-and-error, sometimes using the information about positions of short periodic orbits and their stable and unstable directions. First, one constructs candidate sets, and then modifies them by hand to satisfy certain conditions. This approach is cumbersome and may lead to symbolic dynamics with suboptimal bounds for the topological entropy. In [Bánhelyi *et al.*, 2007], a method to construct candidate sets based on solving a constrained optimization problem via the penalty function approach is discussed. There also exist automatic methods for construction of complex symbolic dynamics based on the construction of isolating neighborhoods, index pairs, and Conley index theory [Szymczak, 1997; Day *et al.*, 2004; Mrozek, 2006; Day *et al.*, 2008]. These methods involve sophisticated mathematical theories, and therefore may be difficult to apply.

In this work, we propose an automatized algorithm to search and prove the existence of complex symbolic dynamics based directly on the method of covering relations. The method starts with the graph representation of the attractor, in which boxes covering the region of interest are graph vertices, and possible transitions between boxes are graph edges. In the first phase of the algorithm, part of the graph is removed, and the invariant part of the remaining graph is used to automatically construct candidates for sets supporting horseshoe type chaos. Then, the existence of symbolic dynamics is proved rigorously using interval arithmetic methods. In this way, we automatically construct quadrangles supporting symbolic dynamics and validate covering relations between them without the necessity of

using Conley index theory tools. Moreover, instead of using exit sets composed of boxes as it is done in [Day *et al.*, 2008], we use one-dimensional quadrangle edges as exit sets, which makes it easier to satisfy conditions for the existence of symbolic dynamics. We also propose a method to reduce the number of symbols and thus to simplify the description of symbolic dynamics without degrading the topological entropy bound.

As an example of the applicability of this method, we study the existence of symbolic dynamics for a simple third-order memristor circuit [Muthuswamy & Chua, 2010]. In [Galias, 2014], it has been shown that the system is chaotic in the topological sense. More precisely, it was proved that symbolic dynamics defined on four symbols with the topological entropy $H \approx 0.3222$ is embedded in the dynamics of the associated return map. Here, using the automatized search method, we construct symbolic dynamics on eight symbols with a larger topological entropy: $H \approx 0.46712$.

The layout of the paper is as follows. In Sec. 2, the notions of topological entropy, symbolic dynamics, and covering relations are briefly recalled. Then, we propose an algorithm for automatized search for complex symbolic dynamics. In Sec. 3, the problem of existence of symbolic dynamics in a return map associated with a simple third-order memristor circuit is studied. Several examples of symbolic dynamics are constructed. We discuss the problem how selection of the part of the attractor to be removed influences the results in terms of the bound of the topological entropy obtained. We show the usefulness of the method by finding lower bounds for the topological entropy better than the bounds known so far.

2. Automatized Method to Search for Complex Symbolic Dynamics

2.1. Topological entropy and symbolic dynamics

Topological entropy quantifies the complexity of the systems by means of calculating the number of trajectories of a given length which can be distinguished under given accuracy. Let us recall a definition of the topological entropy based on the notion of the (n, ε) -separated set [Bowen, 1971]. Let $f: \mathbb{R}^m \mapsto \mathbb{R}^m$ be a continuous map. The set $E \subset X$ is called (n, ε) -separated, if for any points $x, y \in E$, $x \neq y$ there exist $j \in \{0, 1, \dots, n-1\}$ such that the distance between points $f^j(x)$ and $f^j(y)$ is larger than ε . Let $s_n(\varepsilon)$ be the maximum cardinality of an (n, ε) -separated set, i.e. $s_n(\varepsilon) = \max\{\text{card } E: E \text{ is } (n, \varepsilon)\text{-separated}\}$, where $\text{card } E$ denotes the cardinality of the set E . The *topological entropy* of f is defined as

$$H(f) = \lim_{\varepsilon \rightarrow 0} \limsup_{n \rightarrow \infty} \frac{1}{n} \log s_n(\varepsilon). \quad (1)$$

We say that the map is *chaotic in the topological sense* if its topological entropy is positive.

Let us now define what is understood by the existence of symbolic dynamics of a certain type for map f . Let $A = (a_{ij})_{i,j=1}^p$ be a matrix with entries 0 or 1. The *subshift of finite type* with the transition matrix A is the map $\sigma_A = \sigma|_{\Sigma_A}$, where $\sigma: \Sigma_p \mapsto \Sigma_p$ is the shift operator (i.e. $(\sigma(s))_i = s_{i+1}$) defined on the set $\Sigma_p = \{(\dots, s_{-1}, s_0, s_1, s_2, \dots): s_k \in \{1, 2, \dots, p\}\}$ of bi-infinite sequences, and $\Sigma_A = \{s \in \Sigma_p: a_{s_k, s_{k+1}} = 1 \text{ for all } k\}$, The map $\sigma_A = \sigma|_{\Sigma_A}$ is the shift operator restricted to the set Σ_A .

We say that the map f is *semiconjugate with a subshift of finite type* σ_A (or that *for the map f there exist symbolic dynamics with the transition matrix A*) if there exists a homeomorphism $h: \Omega \mapsto \Sigma_A$, with $\Omega \subset \mathbb{R}^m$ such that $h \circ f = \sigma_A \circ h$. The existence of the homeomorphism h means that there is a one-to-one relation between trajectories in Ω and sequences of symbols in Σ_A . The existence of symbolic dynamics means that the dynamics of f is at least as complicated as the dynamics of σ_A .

The following theorem can be used to obtain lower bounds for the topological entropy of f based on the existence of symbolic dynamics [Robinson, 1995].

Theorem 1. *If f is semiconjugate with a subshift with the transition matrix A then the topological entropy $H(f)$ of f is not less than the logarithm of the dominant eigenvalue of A .*

2.2. Covering relations

To prove the existence of symbolic dynamics of a certain type, one can use the method of covering relations. Let us briefly recall the definition and properties of covering relations [Zgliczyński, 1997; Galias & Zgliczyński, 2001] (compare also the notion of windows introduced in [Easton, 1975]). We will limit ourselves to the two-dimensional

case. Let us consider a continuous map $f: \mathbb{R}^2 \mapsto \mathbb{R}^2$. Let us select p pairwise disjoint quadrangles Q_1, Q_2, \dots, Q_p . For each quadrangle we choose two opposite edges and call them “horizontal”. Two other edges are called “vertical”. We say that Q_i f -covers Q_j if (i) the image of Q_i under f is enclosed in the interior of the stripe defined by the horizontal edges of Q_j and (ii) the images of vertical edges of Q_i have empty intersection with Q_j and are located geometrically on the opposite sides of Q_j , i.e. $f(Q_i)$ can be continuously deformed to the set enclosed in the stripe defined by the horizontal edges of Q_j without any intersection with the edges of Q_j and then images of vertical edges of Q_i lie in the stripe on the opposite sides of Q_j .

In the following, instead of standard quadrangles/stripes we will use topological quadrangles/stripes, i.e. sets which can be continuously deformed to quadrangles/stripes. In the example shown in Fig. 1, the quadrangle Q_1 f -covers Q_2 , while the quadrangle Q_2 f -covers both Q_1 and Q_2 .

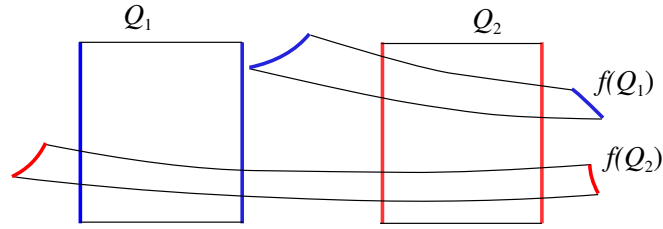


Fig. 1. Covering relation examples. Vertical edges and their images are plotted using thick lines. Q_1 f -covers Q_2 , Q_2 f -covers Q_1 and Q_2 .

Let us now describe how to use covering relations involving a given map f to obtain estimates for the topological entropy of this map. The transition matrix $A = (a_{ij})_{i,j=1}^p$ for the quadrangles Q_1, Q_2, \dots, Q_p is defined by

$$a_{ij} = \begin{cases} 1 & \text{if } Q_i \text{ } f\text{-covers } Q_j, \\ 0 & \text{otherwise.} \end{cases} \quad (2)$$

From the existence of covering relations between quadrangles Q_i described by the transition matrix A , it follows that f is semiconjugate with a subshift with the transition matrix A (compare [Galiás & Zgliczyński, 2001]). Hence, to prove that the topological entropy of f is positive, it is sufficient to show that the logarithm of the dominant eigenvalue of the transition matrix describing covering relations between sets Q_i is positive.

For the standard horseshoe map [Smale, 1967] there are two quadrangles and all four covering relations between them exist. Hence, the transition matrix has all entries equal to one. Since the dominant eigenvalue of the transition matrix is 2, it follows that the topological entropy is $\log 2$. For the example shown in Fig. 1, existing covering relations can be described by the transition matrix

$$A_0 = \begin{pmatrix} 0 & 1 \\ 1 & 1 \end{pmatrix}. \quad (3)$$

The leading eigenvalue of A_0 is $\lambda = (1 + \sqrt{5})/2$ and hence from Theorem 1 it follows that the topological entropy of f is bounded by $H(f) \geq \log \lambda \approx 0.4812$.

2.3. Algorithm to search and prove the existence of complex symbolic dynamics

In this section, we present the algorithm for automatized search for symbolic dynamics and proving the existence of topological chaos. The algorithm will be described for the two-dimensional case. It is possible to extend these method for higher-dimensional state spaces, although for higher dimensions the description of sets supporting symbolic dynamics becomes more complicated.

First, we present the main steps of the algorithm and then describe the algorithm in more detail. The layout of the algorithm to search and prove the existence of symbolic dynamics for the map f is as follows

- (1) Find the graph representation of f .
- (2) Remove some boxes and find the invariant part of the remaining boxes.
- (3) Find eight-connected components.

- (4) Fill holes, “external holes” may also be removed.
- (5) Define polygons Q_i .
- (6) Find exit components of borders ∂Q_i .
- (7) Define quadrangles Q_i .
- (8) Prove the existence of covering relations.
- (9) Remove quadrangles not belonging to cycles of covering relations.
- (10) Optional: simplify the symbolic dynamics description (quadrangle merging).
- (11) Based on the transition matrix compute the lower bound of the topological entropy of f .

In the first step, we find the graph representation of the dynamics of f (compare [Galias, 2001, 2013]). To this end, we cover the region of interest (for example a trapping region or a set enclosing the numerically observed attractor) by ε -boxes, i.e. interval vectors with corners lying on a regular grid: $\mathbf{v} = ([k_1\varepsilon_1, (k_1 + 1)\varepsilon_1], [k_2\varepsilon_2, (k_2 + 1)\varepsilon_2], \dots, [k_m\varepsilon_m, (k_m + 1)\varepsilon_m])$, where k_i are integer numbers, and $\varepsilon = (\varepsilon_1, \varepsilon_2, \dots, \varepsilon_m) \in \mathbb{R}^m$, and m is the dimension of the state space. Next, for each ε -box we compute enclosure of its image under f and find boxes which have non-empty intersection with the enclosure. The set of ε -boxes is the vertex set of the graph and nonforbidden transitions between boxes constitute the edge set.

In the second step, we remove some boxes from the graph. This step is necessary, since the graph obtained in the first step usually has a single connected component, and hence cannot support complex covering relations. This step is the only non-automatic step of the algorithm. The decision which boxes should be removed has to be done by the user. However, in Sec. 3, we will show that the problem of selecting boxes to be removed in order to obtain a good bound of the topological entropy is not very demanding. Generally, it is a good idea to remove a part of the attractor containing a fold. After removing selected boxes, we find the invariant part of the remaining boxes. We remove boxes, which are not the beginning of any edge and boxes which are not the ending of any edge. Removing boxes is continued until no more boxes can be removed from the graph. Additionally, one may remove boxes which do not belong to any cycles, which corresponds to finding the recurrent part of the graph (compare [Galias, 2001]).

Step (2) is carried out to define part of the state space, which supports complex symbolic dynamics. We use a simple method of removing part of the initial set and finding its invariant part. This method was already used in [Galias & Zgliczyński, 2001] as an initial step to define sets supporting symbolic dynamics. There, this step was followed by modification of sets Q_i by hand. Here, we use a fully automatic procedure to define the sets Q_i . There are other options to choose the region of interest, for example growing the set of boxes belonging to low period cycles and their shortest connections (compare [Day *et al.*, 2008]).

In step (3), the set of boxes is divided into eight-connected components. We say that two ε -boxes are eight-connected if they have nonempty intersection, i.e. $\max(|k_1 - l_1|, |k_2 - l_2|) = 1$, where $(k_1, k_2), (l_1, l_2)$ are pairs of integer numbers defining ε -boxes. Finding connected components in a graph is a standard problem in graph theory and has fast solutions with the running time linear in the number of edges and nodes [Gibbons, 1985]. Note that to find connected components one has to redefine graph edges, so that edges correspond to eight-connected boxes. For the existence of complex symbolic dynamics, it is crucial that the number of connected components is at least two. If not, we have to come back to step (2), and use a different criterion to remove boxes. It is also possible to use four-connected components (we say that two ε -boxes are four-connected if their intersection is a segment, i.e. $|k_1 - l_1| + |k_2 - l_2| = 1$). Using eight-connected components is usually better as it reduces the number of components and makes it easier to define quadrangles Q_i . Fig. 2(a) shows one of the eight-connected components produced by the algorithm applied to the system studied in Sec. 3. Note that the leftmost box is not four-connected to other boxes and hence if four-connected components are used this box would define a single-box component.

One can see that the eight-connected component shown in Fig. 2(a) contains two holes which have to be removed before using border of this component to define the quadrangle. Removing holes is carried out in step (4). This is a standard image processing algorithm [Soille, 1999]. One may also use the closing morphological operator with an appropriate structuring element [Soille, 1999] to remove or reduce “external holes”. By an external hole we mean a box which does not belong to a given component and whose three four-connected neighbors are in a given component. One such hole can be seen in Fig. 2(a) above internal holes. Removing external holes is performed to make the borders more smooth.

In step (5) polygons Q_i are defined using border points of eight-connected components found in the previous steps. Defining sets Q_i in this way leads to polygons with right angles between edges. To make the polygon more

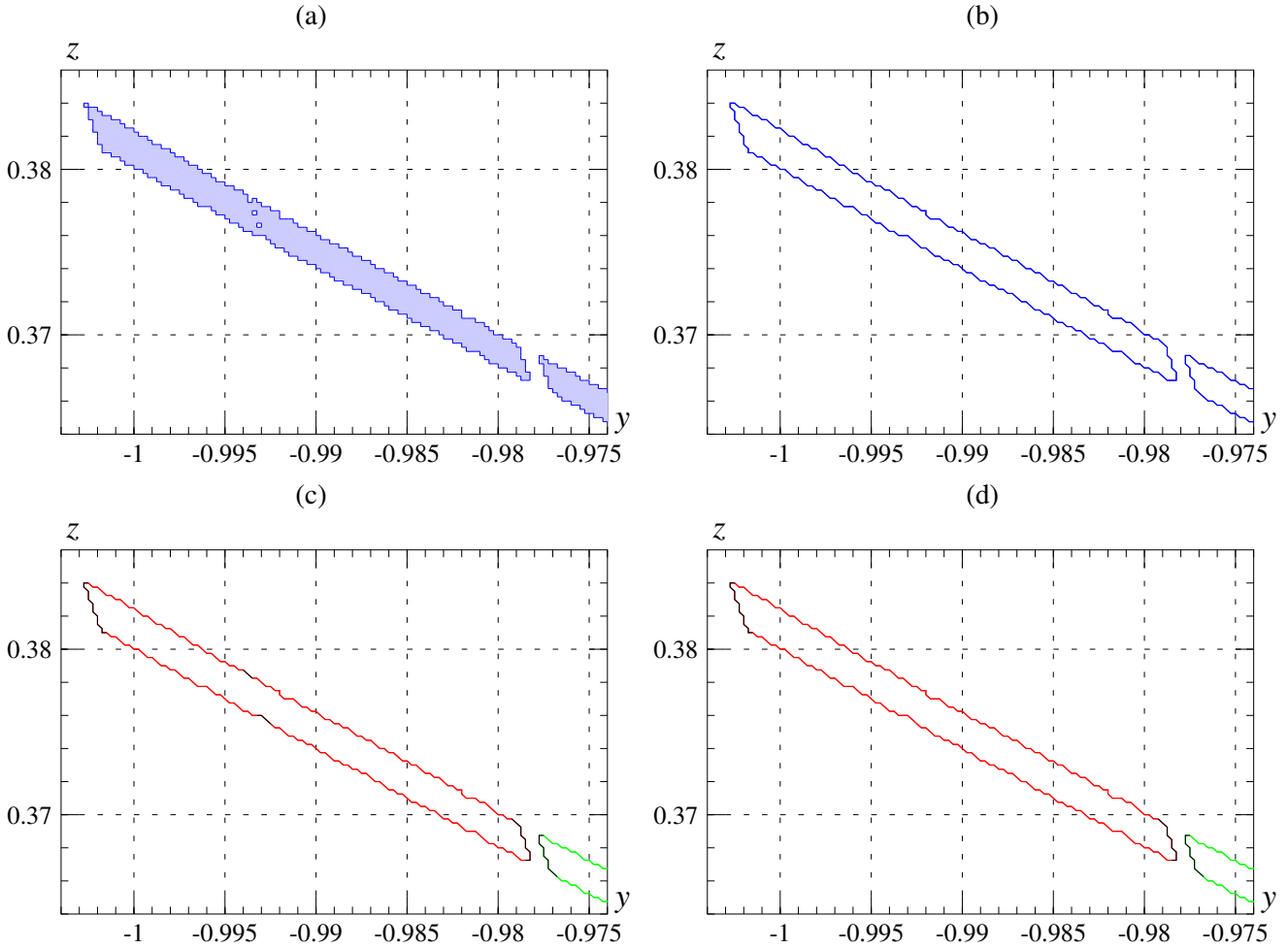


Fig. 2. An example of construction of quadrangles, (a) eight-connected components, (b) holes are removed, polygons are defined, (c) exit components are found, (d) quadrangles are defined

smooth one may remove border points for which the angle is concave (135°). This step is mandatory if a connected component contains boxes which are not four-connected (otherwise the polygon will not be well-defined due to border self-intersections). A polygon obtained from eight-connected components shown in Fig. 2(a) are presented in Fig. 2(b). One can see that due to removing concave border points borders of polygons Q_i become more smooth.

In step (6), for each polygon Q_k we find exit components of its border ∂Q_k . Let us denote by Q the union of polygons Q_i . For each edge $\overline{v_i v_j}$ of Q_k we verify whether $f(\overline{v_i v_j}) \cap Q = \emptyset$. If this is the case, we mark the edge as an exit edge, otherwise the edge is marked as non-exit. The result of this step applied to polygons shown in Fig. 2(b) is presented in Fig. 2(c). Exit edges are denoted using black color. One can see that the red border contains four connected components of exit edges. It is desirable that each border ∂Q_k contains exactly two exit components, as it makes it possible to define a quadrangle Q_k . To reduce the number of exit components, for each exit component we verify whether it has empty intersection with $f(\cup \partial Q_i)$. If this is true then we mark the component as non-exit. The result of this step is shown in Fig. 2(d). One can see that the number of exit components has been reduced to two, as needed. After this step, we have a number of polygons Q_i with two exit components (polygons for which the number of exit sets is not two are deleted).

In step (7) quadrangles Q_i are defined. Exit components of ∂Q_i define vertical edges of Q_i and non-exit components define horizontal edges. Since the number of exit components in each border ∂Q_k is two, quadrangles are properly defined.

In step (8), we prove the existence of covering relations between quadrangles defined in step (7). First, the set of feasible covering relations is found nonrigorously and then each of them is proved independently. In order to prove that Q_i f -covers Q_j it is sufficient to show that (i) the images of horizontal edges of Q_i have empty intersection with

the horizontal edges of Q_j (ii) the images of vertical edges of Q_i have empty intersection with Q_j and (iii), when we move along one of the horizontal edges of Q_i the image is first outside Q_j , then it intersects one of the vertical edges of Q_j , then it is inside Q_j , then it intersects the other vertical edge of Q_j and finally it is outside Q_j . Note that step (8) is the only part of the computations which has to be performed rigorously to ensure that the bound for the topological entropy is correct. There are two options to achieve this goal. The first one is to use non-rigorous computations in all previous steps and carry out rigorous computations involving covering relations in step (8) only. To prove that Q_i f -covers Q_j , edges of Q_i are covered by interval vectors, enclosures of their images are computed rigorously, and conditions listed above are verified. If some of the conditions are not met one can locally use a finer covering and repeat computations. The second options is to start with rigorous computations in step (1) and then use these results in subsequent steps. The first version is faster if the algorithm is performed only once for a given graph representation. This is a consequence of the fact that finding rigorous graph representation is slow and if fact we do not need all the information gathered in this step, since symbolic dynamics is never defined on the whole graph. Moreover, it is faster to prove the existence of covering relations by performing computations on borders of quadrangles only.

In step (9), we remove quadrangles, which do not belong to any cycles of covering relations, and hence have no influence on the complex symbolic dynamics. The transition matrix has to be redefined appropriately. This step is not necessary, it does not change the lower bound of the topological entropy to be obtained. It is performed to reduce the number of symbols.

Step (10) is optional. It is performed to simplify the symbolic dynamics. In this step we attempt to merge pairs of quadrangles. The procedure to merge Q_i and Q_j is as follows. First, it is verified whether the quadrangles are covered by the same quadrangles, i.e. that the columns i and j of the transition matrix are equal. Next, we construct a quadrangle Q_{new} . We identify vertical edges V_i and V_j of quadrangles Q_i and Q_j , which are close to each other. Edges V_i and V_j are removed and the two remaining edges of Q_i and Q_j define vertical edges of Q_{new} . The horizontal edges of Q_{new} are formed by merging corresponding horizontal edges of Q_i and Q_j , adding a segment connecting their ends. We have to make sure that the resulting quadrangle Q_{new} has empty intersection with other quadrangles. Finally, we verify whether the quadrangle Q_{new} covers all quadrangles covered by Q_i and Q_j . If it so, we remove quadrangles Q_i and Q_j and insert the quadrangle Q to the set of quadrangles, and modify the covering matrix accordingly. This step is continued until no quadrangles can be merged. After completion, the topological entropy is the same but the number of quadrangles may be significantly reduced. This will be confirmed in several examples in the following section.

Finally, we compute the leading eigenvalue of the transition matrix obtained in previous steps and the resulting lower bound for the topological entropy using Theorem 1.

3. Analysis of a third order memristor circuit

Let us consider a three element memristor circuit [Muthuswamy & Chua, 2010] shown in Fig. 3. It consist of two linear elements (the capacitor C and the inductor L) and a nonlinear memristor defined by the following equations:

$$\begin{aligned} u_M &= \beta(z^2 - 1)i_M, \\ \frac{dz}{dt} &= i_M - \alpha z - i_M z, \end{aligned}$$

where u_M is the voltage across the device, i_M is the current flowing through the device, and z is the internal variable of the memristor device.

Dynamics of the circuit is described by

$$\begin{aligned} \frac{dx}{dt} &= \frac{y}{C}, \\ \frac{dy}{dt} &= -\frac{1}{L} (x + \beta(z^2 - 1)y), \\ \frac{dz}{dt} &= -y - \alpha z + yz, \end{aligned} \tag{4}$$

where $x(t) = u_C(t)$ is the voltage across the capacitor C , and $y(t) = i_L(t)$ is the current through the inductor L . We will consider the circuit with the following parameter values: $C = 1$, $L = 3$, $\beta = 1.5$, $\alpha = 0.6$.

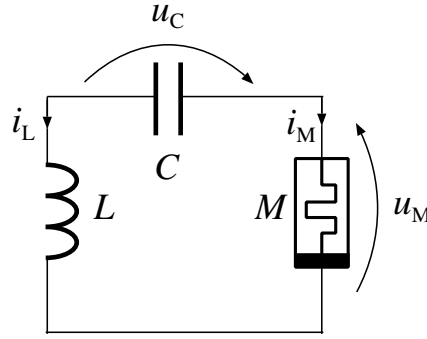
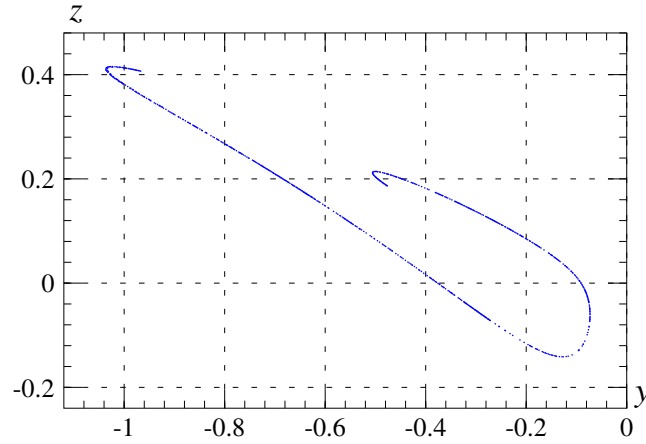


Fig. 3. The Muthuswamy-Chua memristor circuit

Let us choose the return map $P: \Sigma \mapsto \Sigma$ defined by

$$P(x) = \varphi(\tau(x), x), \quad (5)$$

where $\Sigma = \{(x, y, z) \in \mathbb{R}^3: x = 0, \dot{x} < 0\} = \{(x, y, z): x = 0, y < 0\}$, $\varphi(t, x)$ is the trajectory of the system (4) based at x , and $\tau(x) > 0$ is the time needed for the trajectory $\varphi(t, x)$ to reach the section Σ . A trajectory of P composed of 10000 points is shown in Fig. 4.

Fig. 4. A trajectory of the return map P

For the rigorous evaluation of P we use integration methods based on interval arithmetic [Moore, 1979; Alefeld & Herzberger, 1983]. The vector field (4) is integrated using the Taylor integration method of order 30 with automatic control of the time step. The procedure for the rigorous evaluation of the return map P is written using the CAPD library [CAPD]. For details see [Galias, 2014].

In [Galias, 2014], it has been shown that there exists complex symbolic dynamics defined on four quadrangles Q_1 , Q_2 , Q_3 , and Q_4 . The quadrangles and their images computed nonrigorously are shown in Fig. 5. One can see that Q_1 P -covers Q_4 , Q_2 P -covers Q_2 and Q_3 , Q_3 P -covers Q_1 , and Q_4 P -covers Q_2 . The existence of these five coverings have been confirmed. Hence, it has been shown that the following transition matrix

$$A_1 = \begin{pmatrix} 0 & 0 & 0 & 1 \\ 0 & 1 & 1 & 0 \\ 1 & 0 & 0 & 0 \\ 0 & 1 & 0 & 0 \end{pmatrix}. \quad (6)$$

describes a valid symbolic dynamics between the sets Q_i . From Theorem 1 it follows that the topological entropy of

the return map P is not smaller than the dominant eigenvalue of A_1 , i.e.:

$$H(P) \geq 0.3222. \quad (7)$$

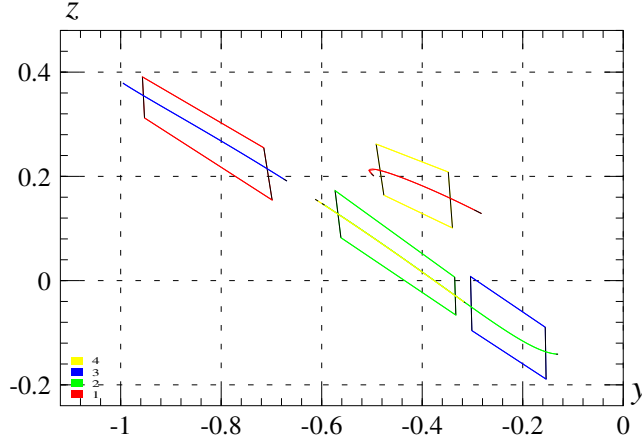


Fig. 5. Borders of quadrangles Q_1, Q_2, Q_3, Q_4 , and their images under P computed nonrigorously

The sets Q_i shown in Fig. 5 have been found by a trial-and-error approach. First, candidate sets have been constructed and then their corners have been moved by hand to satisfy expected covering relations. Below, we present results of application of the algorithm proposed in Sec. 2 to search for sets supporting complex symbolic dynamics for the map P .

As a first step we construct the graph representation of the attractor using ε -boxes of size $\varepsilon = (0.001, 0.001)$. The covering of the attractor is composed of 4455 ε -boxes [see Fig. 6(a)], and there are 43543 edges (nonforbidden connections) in the graph. In the second step, we remove boxes which are enclosed in the region $\{y > y_0\}$, with $y_0 = 0.1$. As it will be shown later, this decision is not crucial for the final result. Many other choices of y_0 lead to symbolic dynamics with the same topological entropy. After this step there are $b_{\text{left}} = 4090$ boxes [shown in Fig. 6(a) using the blue color] connected by 32397 edges. The invariant part of the set of remaining boxes contains $b_{\text{inv}} = 2458$ boxes [see Fig. 6(b)] connected by 17057 edges.

The invariant part is composed of 34 eight-connected components. Three of them are removed because they are very small and as a result we obtain 31 eight-connected components. In the next steps, internal and external holes are removed, border of each component is found, and the smoothing procedure (removing concave border points) is applied. Once polygons Q_i are defined, they are used to define quadrangles. To this end, we identify polygon edges with images located outside $\bigcup Q_i$. Such edges constitute the exit set. We remove from the exit set components which have empty intersection with $f(\bigcup \partial Q_i)$. Each polygon with exactly two exit components defines a quadrangle (exit components define vertical edges).

In this way, we obtain a set of $p_1 = 31$ quadrangles, which is a candidate for a set of quadrangles supporting complex symbolic dynamics. In the last step we have to verify whether this is the case. We prove that there are $n_1 = 47$ covering relations between the quadrangles Q_i . The whole proof required covering of quadrangles' edges by 5320 interval vectors, finding rigorously enclosures of their images under P and verifying certain conditions as described in Sec. 2. The proof took 131 seconds. This is the most time consuming part of the algorithm. Previous steps involve nonrigorous computations and in this particular example could be carried out in a fraction of a second, provided that the graph representation of the attractor is known. Next, the transition matrix is reduced by removing quadrangles not belonging to cycles. As a result we obtain $n_2 = 26$ quadrangles [see Fig. 6(c)] with $p_2 = 41$ covering

Table 2. Performance of the algorithm when boxes enclosed in $\{z > z_0\}$ are removed

z_0	b_{left}	b_{inv}	p_1	n_1	p_2	n_2	p_3	n_3	B
0.21	3279	7	1	1	1	1	1	1	0
0.22	3367	19	3	3	3	3	3	3	0
0.23	3411	19	3	3	3	3	3	3	0
0.24	3456	24	3	3	3	3	3	3	0
0.25	3500	195	15	17	12	15	5	6	0.2406
0.26	3542	383	23	31	20	29	6	9	0.3822
0.27	3586	418	24	35	24	35	4	6	0.4140
0.28	3631	418	24	35	24	35	4	6	0.4140
0.29	3675	418	24	35	24	35	4	6	0.4140
0.30	3721	748	31	45	22	33	4	6	0.4140
0.31	3765	809	31	47	31	47	8	12	0.4421
0.32	3812	966	36	55	31	47	6	9	0.4421
0.33	3857	1186	34	52	30	46	6	9	0.4421
0.34	3903	1372	35	54	30	46	6	9	0.4421
0.35	3950	1434	36	56	30	46	6	9	0.4421
0.36	4001	1767	35	53	26	41	6	9	0.4421
0.37	4054	2062	31	48	24	38	6	9	0.4421
0.38	4105	2291	30	46	23	36	6	9	0.4421
0.39	4159	2442	29	47	26	41	8	13	0.4671
0.40	4213	2442	29	47	26	41	8	13	0.4671
0.41	4313	3846	18	26	7	11	4	6	0.4140
0.42	4455	4455	1	0	0	0	0	0	0

a fixed point belonging to this component. Two other components cover one another, which produces a period-2 orbit. In this case from the existence of symbolic dynamics on three symbols it follows that there exist two periodic orbits. The bound of the topological entropy is zero. In the range $y_0 \in [-0.265, -0.09]$ the bound B is positive, which means that the existence of symbolic dynamics guarantees the existence of infinitely many periodic orbits. Let us note that B is constant over relatively long intervals, for example the maximum value $B = 0.46712$ is observed for $y_0 \in [-0.14, -0.10]$. The case $y_0 = -0.1$ discussed previously in detail belongs to this set. In all cases, the maximum value is realized on $p_2 = 26$ symbols (compare Fig. 6(c)) by $n_2 = 41$ covering relations, which after simplification gives $p_3 = 8$ quadrangles (compare Fig. 6(d)) and $n_3 = 13$ covering relations. Thus, one can see that the choice of the parameter y_0 is not very important for the results obtained. For $y_0 \in \{-0.29, -0.28\}$ the invariant part is composed of $p_1 = 3$ very small eight-connected components built from $b_{\text{inv}} = 19$ boxes. The three components are neighborhoods of period-1 and period-2 orbits. The bound B drops to zero. When $y_0 = -0.3$ the invariant part contains only a neighborhood of the fixed point. It is interesting to note that the lower bound B initially grows when y_0 is decreased (more boxes are removed) until it achieves the maximum value and then it decreases. It follows that it is relatively easy (one may use for example the bisection method) to find the optimal choice of the parameter y_0 for which the maximum is achieved.

Similar computations have been carried out for the case when removed boxes are enclosed in half planes $\{z > z_0\}$ for various values of z_0 . Note that when z_0 is close to 0.4 we remove the fold existing in the upper-left corner of the attractor (compare with Fig. 4). The results are collected in Table 3. General conclusions are the same as for the half planes defined by the condition $\{y > y_0\}$. In particular, the same maximum value of the lower bound B is achieved, which further confirms the statement that the problem of choosing boxes to be removed, which is the only non-automatic part of the search procedure is not very demanding, and can be successfully solved. Note, that the maximum values of B is obtained for $z_0 \in \{0.39, 0.40\}$. This shows that indeed removing part of the attractor containing a fold may be a good choice when searching for complex symbolic dynamics using the presented algorithm.

4. Conclusions

An automatized algorithm to search for sets supporting symbolic dynamics and to find lower bounds of the topological entropy has been proposed. The only decision, which has to be made by the user is the choice of which part of the attractor should be removed. The method has been applied to the analysis of a return map associated with a simple memristor circuit. For this system, symbolic dynamics more complex than the one known so far has been found, thus showing the usefulness of the method. The problem of selecting the region of interest to obtain good lower bounds of topological entropy has been discussed.

In future work, we plan to test other methods to define the region of interest and apply the algorithm for the analysis of other dynamical systems with the goal of improving known lower bounds of topological entropy.

Acknowledgments

This work was supported in part by the AGH University of Science and Technology, grant no. 11.11.120.343.

References

- Alefeld, G. & Herzberger, J. [1983] *Introduction to interval computations* (Academic Press, New York).
- Arioli, G. & Zgliczyński, P. [2001] “Symbolic dynamics for the Hénon-Heiles hamiltonian on the critical energy level,” *J. Diff. Eqs.* **171**, 173–202.
- Bánhelyi, B., Csendes, T. & Garay, B. [2007] “Optimization and the Miranda approach in detecting horseshoe-type chaos by computer,” *Int. J. Bifurcation and Chaos* **17**, 735–747.
- Bowen, R. [1971] “Periodic points and measures for axiom A diffeomorphisms,” *Trans. Amer. Math. Soc.* **154**, 377–397.
- CAPD [2014] “CAPD library,” <http://capd.ii.uj.edu.pl/>.
- Day, S., Frongillo, R. & Trevino, R. [2008] “Algorithms for rigorous entropy bounds and symbolic dynamics,” *SIAM J. Appl. Dyn. Syst.* **1** 1477–1506.
- Day, S., Junge, O. & Mischaikow, K. [2004] “A rigorous numerical method for the global analysis of infinite-dimensional discrete dynamical systems,” *SIAM J. Appl. Dyn. Syst.* **3**, 117–160.
- Easton, R. [1975] “Isolating blocks and symbolic dynamics,” *J. Diff. Eqs.* **17**, 96–118.
- Galias, Z. [1997] “Positive topological entropy of Chua’s circuit: A computer assisted proof,” *Int. J. Bifurcation and Chaos* **7**, 331–349.
- Galias, Z. [2001] “Interval methods for rigorous investigations of periodic orbits,” *Int. J. Bifurcation and Chaos* **11**, 2427–2450.
- Galias, Z. [2013] “The dangers of rounding errors for simulations and analysis of nonlinear circuits and systems—and how to avoid them,” *IEEE Circuits and Systems Magazine* **3**, 35–52.
- Galias, Z. [2014] “Computer assisted proof of chaos in the Muthuswamy-Chua memristor circuit,” *Nonlinear Theory and Its Applications, IEICE E5-N*, to appear.
- Galias, Z. & Zgliczyński, P. [1998] “Computer assisted proof of chaos in the Lorenz equations,” *Physica D* **115**, 165–188.
- Galias, Z. & Zgliczyński, P. [2001] “Abundance of homoclinic and heteroclinic orbits and rigorous bounds for the topological entropy for the Hénon map,” *Nonlinearity* **14**, 909–932.
- Gibbons, A. [1985] *Algorithmic graph theory* (Cambridge University Press, Cambridge).
- Moore, R. [1979] *Methods and applications of interval analysis* (SIAM, Philadelphia).
- Mrozek, M. [2006] “Index pairs algorithms,” *Foundations of Computational Mathematics* **6**, 457–493.
- Muthuswamy, B. & Chua, L. [2010] “Simplest chaotic circuit,” *Int. J. Bifurcation and Chaos* **20**, 1567–1580.
- Robinson, C. [1995] *Dynamical Systems: Stability, Symbolic Dynamics, and Chaos* (CRC Press, USA).
- Smale, S. [1967] “Differentiable dynamical systems,” *Bulletin of the American Mathematical Society* **73**, 747–817.
- Soille, P. [1999] *Morphological Image Analysis: Principles and Applications* (Springer-Verlag).
- Szymczak, A. [1997] “A combinatorial procedure for finding isolating neighborhoods and index pairs,” *Proc. Royal Society of Edinburgh* **127A**, 1075–1088.
- Wilczak, D. [2003] “Chaos in the Kuramoto-Sivashinsky equations — A computer-assisted proof,” *J. Diff. Eqs.* **194**, 433–459.

Zgliczyński, P. [1997] “Computer assisted proof of chaos in the Rössler equations and the Hénon map,” *Nonlinearity*, **10**, 243–252.